Chapter 8

A Robust Induction Motor Control using Sliding Mode Rotor Flux and Load Torque Observers

Oscar Barambones, Patxi Alkorta,
Jose M. Gonzalez de Duran and Jose A. Cortajarena

Additional information is available at the end of the chapter

Abstract

A sliding mode position control for high-performance real-time applications of induction motors is developed in this work. The design also incorporates a sliding mode based flux and load torque observers in order to avoid this sensors, that increases the cost and reduces the reliability. Additionally, the proposed control scheme presents a low computational cost and therefore can be implemented easily in a real-time applications using a low cost DSP-processor.

The stability analysis of the controller under parameter uncertainties and load disturbances is provided using the Lyapunov stability theory. Finally simulated and experimental results show that the proposed controller with the proposed observer provides a good trajectory tracking and that this scheme is robust with respect to plant parameter variations and external load disturbances.

Keywords: Position Control, Sliding Mode Control, Robust Control, Induction Machines, Lyapunov Stability, Nonlinear Control

1. Introduction

AC induction motors have been widely used in industrial applications such machine tools, steel mills and paper machines owing to their good performance provided by their solid architecture, low moment of inertia, low ripple of torque and high initiated torque. Some control techniques have been developed to regulate these induction motor servo drives in high-performance applications. One of the most popular technique is the indirect field oriented control method [1, 2].

The field-oriented technique guarantees the decoupling of torque and flux control commands of the induction motor, so that the induction motor can be controlled linearly as a separated excited D.C. motor. However, the control performance of the resulting linear system is

still influenced by uncertainties, which usually are composed of unpredictable parameter variations, external load disturbances, and unmodelled and nonlinear dynamics.

In the last decades the proportional integral derivative (PID) controller has been widely used in the vector control of induction motors due to its good performance and its simple structure. However in some applications the PID controller may not meet the concerned robustness under parameter variations and external load disturbances. Therefore, many studies have been made on the motor drives in order to preserve the performance under these parameter variations and external load disturbance, such as nonlinear control, multivariable control, optimal control, H-∞ control and adaptive control [3]-[7], etc. However usually these controllers present a high computational cost and cannot be implemented over a low cost DSP processor to perform a real time control.

The sliding-mode control can offer many good properties, such as good performance against unmodelled dynamics, insensitivity to parameter variations, external disturbance rejection and fast dynamic response. These advantages of the sliding-mode control may be employed in the position and speed control of an AC servo system [8]. In [9] an integral sliding mode speed control for induction motor based on field oriented control theory is proposed. In the work of [10], an integrated sliding mode controller (SMC) based on space vector pulse width modulation method is proposed to achieve high-performance speed control of an induction motor. In this work using a field-oriented control principle, a flux SMC is first established to achieve fast direct flux control and then a speed SMC is presented to enhance speed control by the direct torque method. However in this work the performance of the proposed controller is not validated over a real induction motor.

Position control is often used in some applications of electrical drives like robotic systems, conveyor belts, etc. In these applications uncertainty and external disturbances are present and therefore a robust control system that maintain the desired control performance under this situations are frequently required [11]-[15].

The variable structure control strategy using the sliding-mode has also been focussed on many studies and research for the position control of the induction motors [16, 17].

The induction motor position control problem has been studied in [18] using a discrete time sliding mode control. The field oriented control theory is also used in order to decouple the flux and the electromagnetic torque. In this paper the authors calculates the rotor flux vector angular position using the slip estimates which is very sensitive to the rotor resistance variation. In contrast, a rotor flux sliding mode observer is proposed in our control scheme, in order to calculate an accurate value for the angular position of the rotor flux vector in the presence of system uncertainties.

On the other hand in the last decade remarkable efforts have been made to reduce the number of sensors in the control systems [19]-[22]. The sensors increases the cost and also reduces the reliability of the control system because this elements are generally expensive, delicate and difficult to instal.

In this chapter a robust approach for induction motor position control is presented. The proposed sliding mode control may overcome the system uncertainties and load disturbances that usually are present in the real systems. In the controller design, the field oriented control theory is used to simplify the system dynamical equations. Moreover, the proposed controller does not present a high computational cost and therefore can be implemented easily in a real-time applications using a low cost DSP-processor.

In this work a sliding mode flux observer is proposed in order to avoid the flux sensors. The estimated rotor flux is used to calculate the rotor flux vector angular position, whose value is essential in order to apply the field oriented control principle. A load torque estimation algorithm, based on a sliding mode observer, is also presented in order to improve the adaptive robust position control performance. Additionally, the overall control scheme does not involve a high computational cost and therefore can be implemented easily in a real time applications.

Moreover, the control scheme presented in this chapter is validated in a real test using a commercial induction motor of 7.5 kW in order to demonstrate the real performance of this controller. The experimental validation has been implemented using a control platform based on a DS1103 PPC Controller Board that has been designed and constructed in order to carry out the experimental validation of the proposed controller.

This manuscript is organized as follows. The sliding mode flux observer is developed in Section 2 and the sliding mode load torque observer is designed in Section 3. Then, the proposed sliding mode position control is presented in Section 4. In the Section 5, the experimental control platform is presented and some simulation and experimental results are carried out. Finally, concluding remarks are stated in Section 6.

2. Sliding mode observer for rotor flux estimator

Many schemes based on simplified motor models have been devised to estimate some internal variables of the induction motor from measured terminal quantities. This procedure is frequently used in order to avoid the presence of some sensors in the control scheme. In order to obtain an accurate dynamic representation of the motor, it is necessary to base the calculation on the coupled circuit equations of the motor.

Since the motor voltages and currents are measured in a stationary frame of reference, it is also convenient to express the induction motor dynamical equations in this stationary frame.

The system state space equations in the stationary reference frame can be written in the form [23]:

$$\begin{aligned}
\dot{i}_{ds} &= \frac{-1}{\sigma L_s}\left(R_s + \frac{L_m^2}{L_r^2}R_r\right) i_{ds} + \frac{L_m}{\sigma L_s L_r}\frac{1}{T_r}\psi_{dr} \\
&\quad + \frac{L_m}{\sigma L_s L_r} w_r \psi_{qr} + \frac{1}{\sigma L_s} V_{ds} \\
\dot{i}_{qs} &= \frac{-1}{\sigma L_s}\left(R_s + \frac{L_m^2}{L_r^2}R_r\right) i_{qs} - \frac{L_m}{\sigma L_s L_r} w_r \psi_{dr} \\
&\quad + \frac{L_m}{\sigma L_s L_r}\frac{1}{T_r}\psi_{qr} + \frac{1}{\sigma L_s} V_{qs} \\
\dot{\psi}_{dr} &= \frac{L_m}{T_r} i_{ds} - \frac{1}{T_r}\psi_{dr} - w_r \psi_{qr} \\
\dot{\psi}_{qr} &= \frac{L_m}{T_r} i_{qs} + w_r \psi_{dr} - \frac{1}{T_r}\psi_{qr}
\end{aligned} \tag{1}$$

where V_{ds}, V_{qs} are stator voltages; i_{ds}, i_{qs} are stator currents; ψ_{dr}, ψ_{qr} are rotor fluxes; w_r is motor speed; R_s, R_r are stator and rotor resistances; L_s, L_r are stator and rotor inductances; L_m, is mutual inductance; $\sigma = 1 - \frac{L_m^2}{L_s L_r}$ is leakage coefficient; $T_r = \frac{L_r}{R_r}$ is rotor-time constant.

From singular perturbation theory [24], and based on the well-known induction motor model dynamics [23], the slow variables of the system are ψ_{dr}, ψ_{qr} and the fast variables are i_{ds}, i_{qs}. Therefore, the corresponding singularly perturbed model of eqn.(1) is:

$$\begin{aligned}
\varepsilon \dot{i}_{ds} &= -L_m \alpha_r i_{ds} + \alpha_r \psi_{dr} + w_r \psi_{qr} + \frac{L_r}{L_m}\left(V_{ds} - R_s i_{ds}\right) \\
\varepsilon \dot{i}_{qs} &= -L_m \alpha_r i_{qs} - w_r \psi_{dr} + \alpha_r \psi_{qr} + \frac{L_r}{L_m}\left(V_{qs} - R_s i_{qs}\right) \\
\dot{\psi}_{dr} &= L_m \alpha_r i_{ds} - \alpha_r \psi_{dr} - w_r \psi_{qr} \\
\dot{\psi}_{qr} &= L_m \alpha_r i_{qs} + w_r \psi_{dr} - \alpha_r \psi_{qr}
\end{aligned} \tag{2}$$

where $\varepsilon = \frac{\sigma L_s L_r}{L_m}$ and $\alpha_r = \frac{1}{T_r}$.

The proposed sliding mode observer is a copy of the original system model, which has corrector terms with switching functions based on the system outputs. Therefore, considering the measured stator currents as the system outputs, the corresponding sliding-mode-observer can be constructed as follows:

$$\begin{aligned}
\varepsilon \dot{\hat{i}}_{ds} &= -L_m \alpha_r i_{ds} + \alpha_r \hat{\psi}_{dr} + w_r \hat{\psi}_{qr} + \frac{L_r}{L_m}\left(V_{ds} - R_s i_{ds}\right) \\
&\quad -k_1 e_{i_d} + g_{i_d} \operatorname{sgn}(e_{id}) \\
\varepsilon \dot{\hat{i}}_{qs} &= -L_m \alpha_r i_{qs} - w_r \hat{\psi}_{dr} + \alpha_r \hat{\psi}_{qr} + \frac{L_r}{L_m}\left(V_{qs} - R_s i_{qs}\right) \\
&\quad -k_2 e_{iq} + g_{i_q} \operatorname{sgn}(e_{iq}) \\
\dot{\hat{\psi}}_{dr} &= L_m \alpha_r i_{ds} - \alpha_r \hat{\psi}_{dr} - w_r \hat{\psi}_{qr} + g_{\psi_d} \operatorname{sgn}(e_{id}) \\
\dot{\hat{\psi}}_{qr} &= L_m \alpha_r i_{qs} + w_r \hat{\psi}_{dr} - \alpha_r \hat{\psi}_{qr} + g_{\psi_q} \operatorname{sgn}(e_{iq})
\end{aligned} \tag{3}$$

where $\hat{i}$ and $\hat{\psi}$ are the estimations of i and ψ; k_1 and k_2 are positive constant gains; g_{i_d}, g_{i_q}, g_{ψ_d} and g_{ψ_q} are the observer gain matrix; $e_{i_d} = \hat{i}_{ds} - i_{ds}$ and $e_{i_q} = \hat{i}_{qs} - i_{qs}$ are de current errors, and $\operatorname{sgn}()$ is the sign function.

Subtracting eqn.(2) from eqn.(3), the estimation error dynamics are:

$$\begin{aligned}
\varepsilon \dot{\hat{e}}_{i_d} &= \alpha_r e_{\psi_d} + w_r e_{\psi_q} - k_1 e_{i_d} + g_{i_d} \operatorname{sgn}(e_{id}) \\
\varepsilon \dot{\hat{e}}_{i_q} &= -w_r e_{\psi_d} + \alpha_r e_{\psi_q} - k_2 e_{iq} + g_{i_q} \operatorname{sgn}(e_{iq}) \\
\dot{e}_{\psi_d} &= -\alpha_r e_{\psi_d} - w_r e_{\psi_q} + g_{\psi_d} \operatorname{sgn}(e_{id}) \\
\dot{e}_{\psi_q} &= w_r e_{\psi_d} - \alpha_r e_{\psi_q} + g_{\psi_q} \operatorname{sgn}(e_{iq})
\end{aligned} \tag{4}$$

where $e_{\psi_d} = \hat{\psi}_{dr} - \psi_{dr}$, $e_{\psi_q} = \hat{\psi}_{qr} - \psi_{qr}$

The previous equations can be expressed in matrix form as:

$$\begin{aligned} \varepsilon \dot{e}_i &= +Ae_\psi + K_i e_i + G_i \mathrm{Y}_e \\ \dot{e}_\psi &= -Ae_\psi + G_\psi \mathrm{Y}_e \end{aligned} \tag{5}$$

where $A = \alpha_r I_2 - w_r J_2$, $e_i = [e_{i_d}\ e_{i_q}]^T$, $e_\psi = [e_{\psi_d}\ e_{\psi_q}]^T$, $\mathrm{Y}_e = [\mathrm{sgn}(e_{id})\ \mathrm{sgn}(e_{iq})]^T$,

$G_i = \begin{bmatrix} g_{i_d} & 0 \\ 0 & g_{i_q} \end{bmatrix}, G_\psi = \begin{bmatrix} g_{\psi_d} & 0 \\ 0 & g_{\psi_q} \end{bmatrix}$

$I_2 = \begin{bmatrix} 1 & 0 \\ 0 & 1 \end{bmatrix}, J_2 = \begin{bmatrix} 0 & -1 \\ 1 & 0 \end{bmatrix}, K_i = \begin{bmatrix} -k_1 & 0 \\ 0 & -k_2 \end{bmatrix}$

Following the two-time-scale approach, the stability analysis of the above system can be considered determining the observer gains G_i and K_i of the fast subsystem or measured state variables (i_{ds}, i_{qs}), to ensure the attractiveness of the sliding surface $e_i = 0$ in the fast time scale. Thereafter, the observer gain G_ψ of the slow subsystem or inaccessible state variables (ψ_{dr}, ψ_{qr}), are determined, such that the reduced-order system obtained when $e_i \cong \dot{e}_i \cong 0$ is locally stable [24].

From singular perturbation theory, the fast reduced-order system of the observation errors can be obtained by introducing the new time variable $\tau = (t - t_0)/\varepsilon$ and thereafter setting $\varepsilon \to 0$ [24]. In the new time scale τ, taking into account that $d\tau = dt/\varepsilon$, eqn.(5) becomes:

$$\begin{aligned} \frac{d}{d\tau} e_i &= Ae_\psi + K_i e_i + G_i \mathrm{Y}_e \\ \frac{d}{d\tau} e_\psi &= 0 \end{aligned} \tag{6}$$

Therefore, if the observer gains G_i and K_i are adequately chosen, the sliding mode occurs in eqn.(6) along the manifold $e_i = [e_{i_d}\ e_{i_q}]^T = 0$.

The attractivity condition of the sliding surface $e_i = 0$ given by:

$$e_i^T \frac{de_i}{d\tau} < 0 \tag{7}$$

is fulfilled with the following inequalities,

$$g_{i_d} < -\left|\alpha_r e_{\psi_d} + w_r e_{\psi_q}\right| - k_1 \left|e_{id}\right| \tag{8}$$

$$g_{i_q} < -\left|-w_r e_{\psi_d} + \alpha_r e_{\psi_q}\right| - k_2 \left|e_{iq}\right| \tag{9}$$

Proof:

Let us define the following Lyapunov function candidate,

$$V = \frac{1}{2} e_i^T e_i$$

whose time derivative is,

$$\begin{aligned} \frac{dV}{d\tau} &= e_i^T \frac{de_i}{d\tau} \\ &= e_i^T \left[A e_\psi + K_i e_i + G_i \mathrm{Y}_e \right] \\ &= \begin{bmatrix} e_{id} \left\{ g_{i_d} \operatorname{sgn}(e_{id}) + \alpha_r e_{\psi_d} + w e_{\psi_q} - k_1 e_{id} \right\} \\ e_{iq} \left\{ g_{i_q} \operatorname{sgn}(e_{iq}) - w e_{\psi_d} + \alpha_r e_{\psi_q} - k_2 e_{iq} \right\} \end{bmatrix} \end{aligned} \tag{10}$$

Taking into account that all states and parameters of induction motor are bounded, then there exist sufficiently large negative numbers g_{i_d}, g_{i_q}, and positive numbers k_1 and k_2 so that the inequalities defined in eqn.(9) are verified and then the attractivity condition defined in eqn.(7) is fulfilled.

Then, once the currents trajectory reaches the sliding surface $e_i = 0$, the observer error dynamics given by eqn.(6) behaves, in the sliding mode, as a reduced-order subsystem governed only by the rotor-flux error e_ψ, assuming that $e_i = \dot{e}_i = 0$.

The slow error dynamics (when $e_i = 0$ and $\dot{e}_i = 0$), can be obtained setting $\varepsilon = 0$ in the system equation presented in eqn.(5):

$$\begin{aligned} 0 &= +A e_\psi + G_i \mathrm{Y}_e \\ \dot{e}_\psi &= -A e_\psi + G_\psi \mathrm{Y}_e \end{aligned} \tag{11}$$

In order to demonstrate de stability of the previous system, the following Lyapunov function candidate is proposed:

$$V = \frac{1}{2} e_\psi^T e_\psi \tag{12}$$

The time derivative of the Lyapunov function candidate is:

$$\frac{dV}{dt} = \dot{e}_\psi^T e_\psi \tag{13}$$

From eqn.(11) it is deduced that:

$$e_\psi = -A^{-1}G_i\mathrm{Y}_e \tag{14}$$
$$\dot{e}_\psi = (G_i + G_\psi)\mathrm{Y}_e \tag{15}$$

Then from eqn.(13), (14) and (15)

$$\begin{aligned}
\frac{dV}{dt} &= -\mathrm{Y}_e^T(G_i + G_\psi)^T A^{-1}G_i\mathrm{Y}_e \\
&= -\mathrm{Y}_e^T(G_i + G_\psi)^T A^{-1}G_i\mathrm{Y}_e \\
&= -\mathrm{Y}_e^T\left[(I_2 + G_\psi G_i^{-1})G_i\right]^T A^{-1}G_i\mathrm{Y}_e \\
&= -\mathrm{Y}_e^T G_i^T(I_2 + G_\psi G_i^{-1})^T A^{-1}G_i\mathrm{Y}_e \\
&= -\mathrm{Y}_e^T G_i^T(A^{-1})^T A^T(I_2 + G_\psi G_i^{-1})^T A^{-1}G_i\mathrm{Y}_e \\
&= -(A^{-1}G_i\mathrm{Y}_e)^T A^T(I_2 + G_\psi G_i^{-1})^T A^{-1}G_i\mathrm{Y}_e \\
&= -e_\psi^T A^T(I_2 + G_\psi G_i^{-1})^T e_\psi \\
&= -e_\psi^T(I_2 + G_\psi G_i^{-1})A\, e_\psi
\end{aligned} \tag{16}$$

To ensure that $\dot{V}$ is negative definite the following sufficient condition can be requested:

$$(I_2 + G_\psi G_i^{-1})A \geq \varrho I_2 \tag{17}$$

where ϱ is a positive constant

Solving the gain matrix G_ψ in eqn.(17) yields:

$$(I_2 + G_\psi G_i^{-1}) \geq \varrho I_2 A^{-1} \tag{18}$$
$$(I_2 + G_\psi G_i^{-1}) \geq \varrho A^{-1} \tag{19}$$
$$G_\psi G_i^{-1} \geq \varrho A^{-1} - I_2 \tag{20}$$
$$G_\psi \leq (\varrho A^{-1} - I_2)G_i \tag{21}$$

Therefore, the time derivative of the Lyapunov function will be negative definite if the observer gain G_ψ is chosen taking into account eqn.(21). As a result from eqn.(16) it is concluded that the equilibrium point ($e_\psi = 0$) of the flux observer error dynamic given by eqn.(11) is exponentially stable; that is, the flux observer error converges to zero with exponential rate of convergence.

3. Load Torque Observer

In the traditional sliding mode control schemes, the load torque should be known or should be measured using a torque sensors in order to compensate this load torque. On the other hand, the load torque could be also considered as a system uncertainty, but in this case the control system should be robust under all load torque values that would appear over the time and therefore the sliding gain should be adequately high in order to compensate the these load torque values. Obviously these high values for the sliding gain will increase the control activity and are undesirable in the real applications.

Therefore, when the load torque is unknown or is very variable over time, and the system has no torque sensors, a good solution could be the use of a load torque estimator. In this chapter a sliding mode observer is proposed in order to obtain the load torque applied to the induction motor without requiring the use of the load torque sensor.

The mechanical equation of an induction motor can be written as:

$$J\ddot{\theta}_m + B\dot{\theta}_m + T_L = T_e \tag{22}$$

where J and B are the inertia constant and the viscous friction coefficient of the induction motor respectively; T_L is the external load; θ_m is the rotor mechanical position, which is related to the rotor electrical position, θ_r, by $\theta_m = 2\,\theta_r / p$ where p is the pole numbers and T_e denotes the generated torque of an induction motor, defined as [23]:

$$T_e = \frac{3p}{4}\frac{L_m}{L_r}(\psi^e_{dr} i^e_{qs} - \psi^e_{qr} i^e_{ds}) \tag{23}$$

where ψ^e_{dr} and ψ^e_{qr} are the rotor-flux linkages, with the subscript 'e' denoting that the quantity is referred to the synchronously rotating reference frame; i^e_{ds} and i^e_{qs} are the d-q stator current components, and p is the pole numbers.

The relation between the synchronously rotating reference frame and the stationary reference frame is performed by the so-called reverse Park's transformation:

$$\begin{bmatrix} x_a \\ x_b \\ x_c \end{bmatrix} = \begin{bmatrix} \cos(\theta_e) & -\sin(\theta_e) \\ \cos(\theta_e - 2\pi/3) & -\sin(\theta_e - 2\pi/3) \\ \cos(\theta_e + 2\pi/3) & -\sin(\theta_e + 2\pi/3) \end{bmatrix} \begin{bmatrix} x^e_d \\ x^e_q \end{bmatrix} \tag{24}$$

where θ_e is the angular position between the d-axis of the synchronously rotating reference frame and the a-axis of the stationary reference frame, and it is assumed that the quantities are balanced.

Using the field-orientation control principle, the current component i^e_{ds} is aligned in the direction of the rotor flux vector $\bar{\psi}_r$, and the current component i^e_{qs} is aligned in the perpendicular direction to it. At this condition, it is satisfied that:

$$\psi^e_{qr} = 0, \qquad \psi^e_{dr} = |\bar{\psi}_r| \tag{25}$$

Taking into account the results presented in eqn.(25), the induction motor torque of eqn.(23) is simplified to:

$$T_e = \frac{3p}{4}\frac{L_m}{L_r}\psi_{dr}^e i_{qs}^e = K_T\, i_{qs}^e \tag{26}$$

where K_T is the torque constant, defined as follows:

$$K_T = \frac{3p}{4}\frac{L_m}{L_r}\psi_{dr}^{e^*} \tag{27}$$

where $\psi_{dr}^{e^*}$ denotes the command rotor flux.

With the above mentioned proper field orientation, the rotor flux dynamics is given by [23]:

$$\frac{d\psi_{dr}^e}{d\,t} + \frac{\psi_{dr}^e}{T_r} = \frac{L_m}{T_r}\, i_{ds}^e \tag{28}$$

From the system mechanical equation eqn.(22) and the induction motor torque equation eqn.(26), the following dynamic equation is obtained:

$$\dot{w}_m = -\frac{B}{J}w_m + \frac{K_T}{J}\, i_{qs}^e - \frac{1}{J}T_L \tag{29}$$

where $w_m = \dot{\theta}_m$

It is assumed that the load torque only changes at certain moments, and therefore the load torque can be considered as a quasi-constant signal:

$$\dot{T}_L = 0 \tag{30}$$

Therefore, the system state space equations are:

$$\begin{aligned} \dot{w}_m &= -\frac{B}{J}w_m + \frac{K_T}{J}\, i_{qs}^e - \frac{1}{J}T_L \\ \dot{T}_L &= 0 \end{aligned} \tag{31}$$

Taking into account that the load torque T_L is taken as a quasi-constant signal, the load torque can be considered the slow component of this system. Therefore, from singular perturbation theory [24], the stability of the above system can be demonstrated assuring the asymptotic stability of the fast component of this system (the rotor speed), and thereafter the convergence of the slow component (the load torque) for the reduced system, when the rotor speed estimation error is zero.

Then, from eqn.(31) the sliding-mode-observer can be constructed as:

$$\begin{aligned}\dot{\hat{w}}_m &= \frac{-B}{J} w_m + \frac{K_T}{J} i_{qs}^e - \frac{1}{J}\hat{T}_L + k_{w_1} e_w + h_1 \operatorname{sgn}(e_w) \\ \dot{\hat{T}}_L &= -k_{w_2} e_w - h_2 \operatorname{sgn}(e_w)\end{aligned} \tag{32}$$

where $e_w = w_m - \hat{w}_m$, and k_{w_1}, k_{w_2}, h_1 and h_2 are a positive constants.

Subtracting eqn. (32) from (31), the estimation error dynamic is obtained:

$$\begin{aligned}\dot{e}_w &= -\frac{1}{J} e_T - k_{w_1} e_w - h_1 \operatorname{sgn}(e_w) \\ \dot{e}_T &= k_{w_2} e_w + h_2 \operatorname{sgn}(e_w)\end{aligned} \tag{33}$$

where $e_T = T_L - \hat{T}_L$

In order to demonstrate the stability of the fast component of the system the following Lyapunov function candidate is proposed:

$$V = \frac{1}{2} e_w^2 \tag{34}$$

The time derivative of this Lyapunov function candidate is:

$$\dot{V} = e_w \dot{e}_w \tag{35}$$

$$= e_w \left(-\frac{1}{J} e_T - k_{w_1} e_w - h_1 \operatorname{sgn}(e_w) \right) \tag{36}$$

$$= -h_1 |e_w| - k_{w_1} e_w^2 - \frac{1}{J} e_w e_T \tag{37}$$

To ensure that $\dot{V}$ is negative definite the following sufficient condition can be requested:

$$h_1 \geq \left| \frac{1}{J} e_T \right| - k_{w_1} |e_w| + \eta_w \tag{38}$$

where $\eta_w > 0$

Therefore,

$$\dot{V} \leq -\eta_w |e_w| \tag{39}$$

From eqn.(39) it is deduced that the equilibrium point $e_w = 0$ is asymptotically stable, and from this equation it can be also deduced that the maximum time in order to reach the equilibrium point $e_w = 0$ is:

$$t_{reach} \leq \frac{e_w(t=0)}{\eta_w} \tag{40}$$

When the speed observation error reaches the equilibrium point, $e_w = 0$ and $\dot{e}_w = 0$, and then from eqn.(33) it is obtained that the observer error dynamics behaves as the reduced-order subsystem presented below:

$$0 = -\frac{1}{J} e_L - h_1 \operatorname{sgn}(e_w) \tag{41}$$

$$\dot{e}_T = h_2 \operatorname{sgn}(e_w) \tag{42}$$

From the previous equations it is obtained:

$$\dot{e}_T = -\frac{1}{J} \frac{h_2}{h_1} e_T \tag{43}$$

The solution of the previous differential equation is:

$$e_T(t) = C \exp\left(-\frac{1}{J} \frac{h_2}{h_1} t\right) \tag{44}$$

Consequently, the load torque estimation error tends exponentially to zero.

Therefore, if the observer gains h_1, h_2 k_{w_1} and k_{w_2} are adequately chosen, then the estimation error converges to zero. Consequently the estimated states $\hat{w}_m$, $\hat{T}_L$ converges to the real states w_m, T_L as t tends to infinity. Hence, the load torque may be obtained from the states observer given by eqn.(32), that uses the rotor speed and the stator current in order to obtain the load torque applied to the induction motor.

4. Variable structure robust position control

The mechanical equation of an induction motor presented in equation (29) can be rewritten as:

$$\ddot{\theta}_m + a\,\dot{\theta}_m + \bar{f} = b\, i^e_{qs} \tag{45}$$

where the parameters are defined as:

$$a = \frac{B}{J}, \quad b = \frac{K_T}{J}, \quad \bar{f} = \frac{T_L}{J}; \tag{46}$$

Now, the previous mechanical equation (45) is considered with uncertainties as follows:

$$\ddot{\theta}_m = -(a + \triangle a)\dot{\theta}_m - (f + \triangle f) + (b + \triangle b)i_{qs}^e \tag{47}$$

where $f = \frac{\hat{T}_L}{J}$, and the terms $\triangle a$, $\triangle b$ and $\triangle f$ represents the uncertainties of the terms a, b and f respectively.

It should be noted that the load torque T_L has been replaced by the estimated load torque $\hat{T}_L$ and the difference between the real and the estimated value is taken as an uncertainty.

Let us define the position tracking error as follows:

$$e(t) = \theta_m(t) - \theta_m^*(t) \tag{48}$$

where θ_m^* is the rotor position command.

Taking the second derivative of the previous equation with respect to time yields:

$$\ddot{e}(t) = \ddot{\theta}_m - \ddot{\theta}_m^* = u(t) + d(t) \tag{49}$$

where the following terms have been collected in the signal $u(t)$,

$$u(t) = b\, i_{qs}^e(t) - a\, \dot{\theta}_m(t) - f(t) - \ddot{\theta}_m^*(t) \tag{50}$$

and the uncertainty terms have been collected in the signal $d(t)$,

$$d(t) = -\triangle a\, w_m(t) - \triangle f(t) + \triangle b\, i_{qs}^e(t) \tag{51}$$

Now, the sliding variable $S(t)$ is defined as:

$$S(t) = \dot{e}(t) + k\, e(t) + k_i \int e(t)\, dt \tag{52}$$

where k and k_i are a positive constant gains.

Then, the sliding surface is defined as:

$$S(t) = \dot{e}(t) + k\, e(t) + k_i \int e(t)\, dt = 0 \tag{53}$$

The sliding mode controller is designed as:

$$u(t) = -k\,\dot{e} - k_i\,e - \beta\,\mathrm{sgn}(S) \tag{54}$$

where k and k_i are the previously defined positive constant gains, β is the switching gain, S is the sliding variable defined in eqn. (52) and $\mathrm{sgn}(\cdot)$ is the sign function.

Assumption. In order to obtain the position trajectory tracking, the gain β must be chosen so that $\beta \geq \bar{d}$ where $\bar{d} \geq \sup_{t \in R^{0+}} |d(t)|$. Note that this condition only implies that the system uncertainties are bounded magnitudes.

Theorem. Consider the induction motor given by equation (47), the control law (54) leads the rotor mechanical position $\theta_m(t)$ so that the position tracking error $e(t) = \theta_m(t) - \theta_m^*(t)$ tends to zero as the time tends to infinity.

Proof: Define the Lyapunov function candidate:

$$V(t) = \frac{1}{2} S(t) S(t) \tag{55}$$

Its time derivative is calculated as:

$$\begin{aligned}
\dot{V}(t) &= S(t)\dot{S}(t) \\
&= S \cdot [\ddot{e} + k\,\dot{e} + k_i\,e] \\
&= S \cdot [u + d + k\,\dot{e} + k_i\,e] \\
&= S \cdot [-k\,\dot{e} - k_i\,e - \beta\,\mathrm{sgn}(S) + d + k\,\dot{e} + k_i\,e] \\
&= S \cdot [d - \beta\,\mathrm{sgn}(S)] \\
&\leq -(\beta - |d|)|S| \\
&\leq 0
\end{aligned} \tag{56}$$

It should be noted that the eqns. (52), (49) and (54) have been used in the proof.

Using the Lyapunov's direct method, since $V(t)$ is clearly positive-definite, $\dot{V}(t)$ is negative definite and $V(t)$ tends to infinity as $S(t)$ tends to infinity, then the equilibrium at the origin $S(t) = 0$ is globally asymptotically stable. Therefore $S(t)$ tends to zero as the time t tends to infinity. Moreover, all trajectories starting off the sliding surface $S = 0$ must reach it in finite time and then they will remain on this surface. This system's behavior, once on the sliding surface is usually called *sliding mode*.

When the sliding mode occurs on the sliding surface (53), then $S(t) = \dot{S}(t) = 0$, and therefore the dynamic behavior of the tracking problem (49) is equivalently governed by the following equation:

$$\dot{S}(t) = 0 \quad \Rightarrow \quad \ddot{e}(t) + k\,\dot{e}(t) + k_i e(t) = 0 \tag{57}$$

Then, like k and k_i are a positive constants, the tracking error $e(t)$ and its derivatives $\dot{e}(t)$ and $\ddot{e}(t)$ converges to zero exponentially.

It should be noted that, a typical motion under sliding mode control consists of a *reaching phase* during which trajectories starting off the sliding surface $S = 0$ move toward it and reach it in finite time, followed by *sliding phase* during which the motion will be confined to this surface and the system tracking error will be represented by the reduced-order model (57), where the tracking error tends to zero.

Finally, the torque current command, $i_{qs}^{e*}(t)$, can be obtained directly substituting eqn. (54) in eqn. (50):

$$i_{qs}^{e*}(t) = \frac{1}{b}\left[-k\,\dot{e} - k_i\,e - \beta\,\mathrm{sgn}(S) + a\,\dot{\theta}_m + \ddot{\theta}_m^* + f(t)\right] \tag{58}$$

It should be noted that the current command is a bounded signal because all its components are bounded.

Therefore, the proposed variable structure position control resolves the position tracking problem for the induction motor in presence of some uncertainties in mechanical parameters and load torque.

It should be pointed out that, as it is well known, the variable structure control signals may produce the so-called chattering phenomenon, caused by the discontinuity that appear in eqn.(58) across the sliding surface. Chattering is undesirable in practice, since it involves high control activity and further may excite high-frequency dynamics. However, in the induction motor system, this high frequency changes in the electromagnetic torque will be filtered by the mechanical system inertia. Nevertheless, in order to reduce the chattering effect, the control law can also be smoothed out. In this case a simple and easy solution (proposed in [25]) could be to replace the sign function by a tansigmoid function in order to avoid the discontinuity in the control signal.

5. Simulation and Experimental Results

In this section the position regulation performance of the proposed sliding-mode field oriented control versus reference and load torque variations is analyzed by means of different simulation examples and real test using a commercial induction motor.

The block diagram of the proposed robust position control scheme is presented in Figure 1, and the function of the blocks that appear in this figure are explained below:

The block 'SMC Controller' represents the proposed sliding-mode controller, and it is implemented by equations (52) and (58). The block 'limiter' limits the current applied to the motor windings so that it remains within the limit value, being implemented by a saturation function. The block '$dq^e \rightarrow abc$' makes the conversion between the synchronously rotating

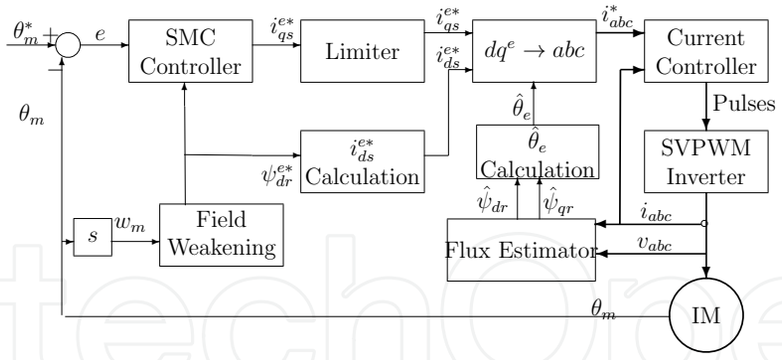

Figure 1. Block diagram of the proposed sliding-mode field oriented control

and stationary reference frames (Park's Transformation). The block 'Current Controller' consists of a SVPWM current control. The block 'SVPWM Inverter' is a six IGBT-diode bridge inverter with 540 V DC voltage source. The block 'Field Weakening' gives the flux command based on rotor speed, so that the PWM controller does not saturate. The block 'i_{ds}^{e*} Calculation' provides the current reference i_{ds}^{e*} from the rotor flux reference through the equation (28). The block 'Flux Estimator' represents the proposed sliding mode flux estimator, and it is implemented by the eqn.(3). The block '$\hat{\theta}_e$ Calculation' provides the angular position of the rotor flux vector. Finally, the block 'IM' represents the induction motor.

In order to carry out the real experimental validation of the proposed control scheme, the control platform show in figure 2 is used . The block diagram of this experimental platform is shown in figure 3.

This control platform allows to verify the real time performance of the induction motor controls in a real induction motor. The platform is formed by a PC with Windows XP in which it is installed MatLab7/Simulink R14 and ControlDesk 2.7 and the DS1103 Controller Board real time interface of dSpace. The power block is formed of a three-phase rectifier connected to 380 V/50 Hz AC electrical net and a capacitor bank of 27.200 μF in order to get a DC bus of 540 V. The platform also includes a three-phase IGBT/Diode bridge of 50A, and the M2AA 132M4 ABB induction motor of 7.5kW of die-cast aluminium squirrel-cage type and 1440 rpm, with the following parameters given by the manufacturer:

- w_N, nominal speed, 1440 rpm
- T_N, nominal torque, 49.3 Nm
- R_s, stator resistance, 0.81 Ω
- R_r, rotor resistance, 0.57 Ω
- L_m, magnetizing inductance, 0.118 mH
- L_s, stator inductance, 0.120 mH
- L_r, rotor inductance, 0.122 mH
- p, pair of poles, 2
- J, moment of inertia, 0.057 $kg\,m^2$
- B, viscous friction coefficient, 0.015 $N\,m/(rad/s)$

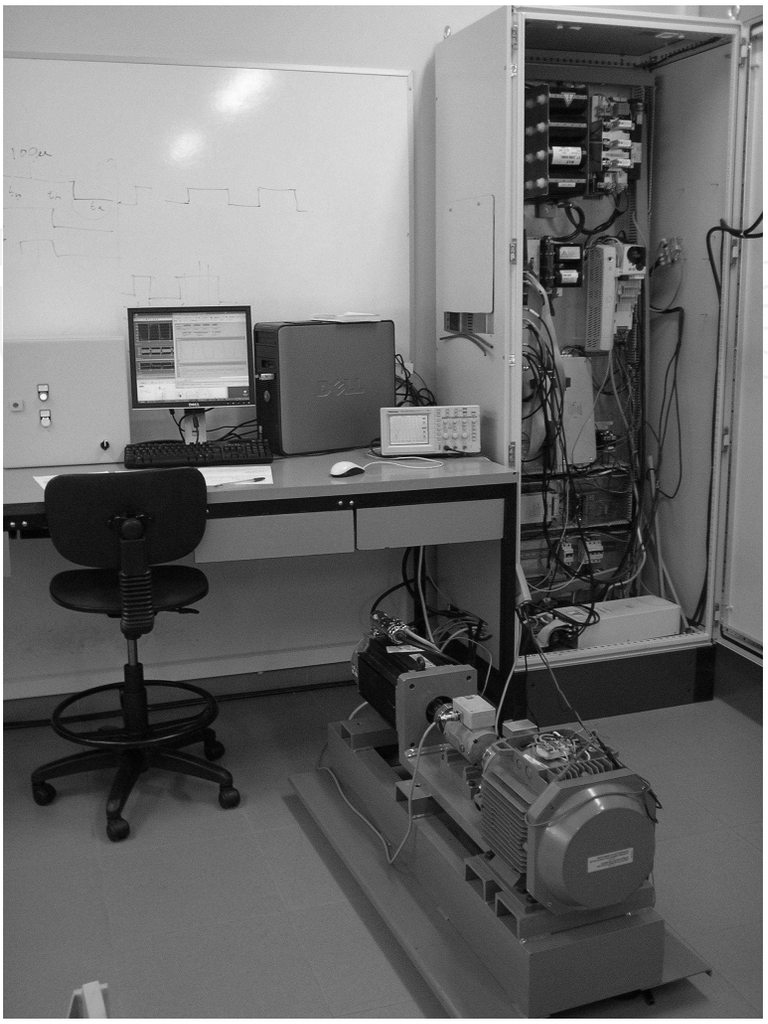

Figure 2. Induction motor experimental platform

- α_{Al}, temperature coefficient of Aluminium, $0.0039K^{-1}$

The rotor position of this motor is measured using the G1BWGLDBI LTN incremental rotary encoder of 4096 square impulses per revolution. This pulses are quadruplicated in a decoder, giving a resolution of 16384 ppr which gives an angle resolution of 0.000385 rad (0.022 deg).

The platform also includes a 190U2 Unimotor synchronous AC servo motor of 10.6 kW connected to the induction motor to generate the load torque (controlled in torque). This servo motor is controlled by its VSI Unidrive inverter module.

The sample time used to realize the real implementation of the the position control is $100\mu s$, and the processor used for the real tests is a floating point PowerPC at 1MHz, located in the real time DS1103 hardware of dSpace. This target incorporates the TMS320F240 DSP working as slave to generate the SVPWM pulses for the inverter. Finally, the position and currents control algorithms, the θ_e angle and flux estimator, the SVPWM calculations, and the Park's transformations have been realized in C programming language in a unique S-Builder module of Simulink, in order to obtain a compact and portable code.

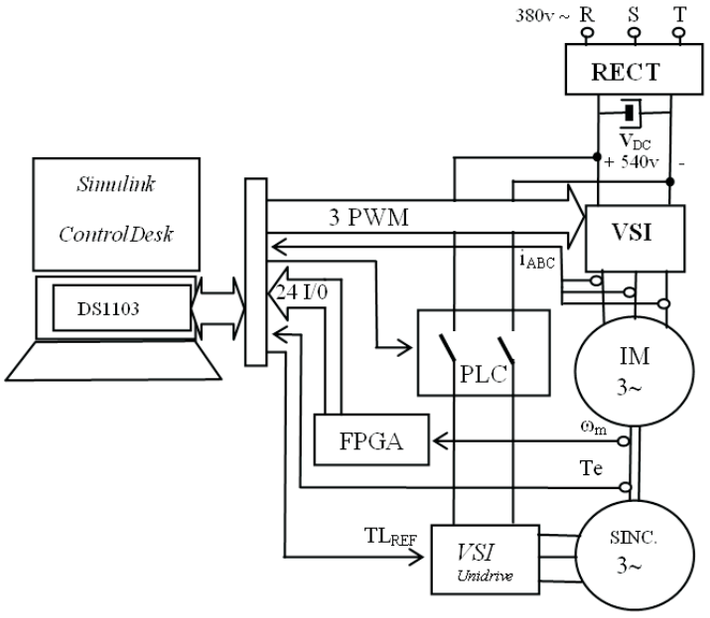

Figure 3. Block diagram of the induction motor experimental platform

In the experimental validation it is assumed that there is an uncertainty around 50% in the system mechanical parameters, that will be overcome by the proposed sliding mode control. The nominal value of the rotor flux is 1.01 Wb and it is obtained for a flux current command value of $i_{sd}^{*} = 8.61A$. However, in some cases, for a very high rotor speed, the flux command should be reduced so that the PWM controller does not saturate.

On the other hand, the electromagnetic torque current command, i_{sq}^{*}, has been limited to 30 A, in order to provide a protection against overcurrents in the induction motor's stator feed. Finally, the frequency of commutation of VSI module of the platform is limited to 8 kHz.

In this example the motor starts from a standstill state and it is required that the rotor position follows a position command, whose amplitude varies between 0 and $2\pi\, rad$.

The system starts with an initial load torque $T_L = 0\, N.m$, and at time $t = 0.1\, s$, the load torque steps from $T_L = 0\, N.m$ to $T_L = 20\, N.m$, then at time $t = 1\, s$, the load torque steps from $T_L = 20\, N.m$ to $T_L = 40\, N.m$ and finally at time $t = 2\, s$, the load torque steps from $T_L = 40\, N.m$ to $T_L = 60\, N.m$, which is a 20% above the nominal torque value (49 Nm).

In these examples the values for the controller parameters are: $k = 46$, $k_i = 160$ and $\beta = 20$, the values for the flux observer parameters are: $g_{i_d} = -44.5$, $g_{i_q} = -44.5$, $g_{\psi_d} = -50$, $g_{\psi_q} = -50$, $k_1 = 100$ and $k_2 = 100$, and the values for the load torque observer parameters are: $k_{w_1} = 25$, $k_{w_2} = 250$ $h_1 = 100$ and $h_2 = 100$.

Figure 4 shows the simulation test of the proposed adaptive variable structure position control. The first graph shows the reference and the real rotor position, and the second graph shows the rotor position error. As it can be observed, after a transitory time in which the sliding gain is adapted, the rotor position tracks the desired position in spite of system uncertainties. Nevertheless, at time $t = 1s$ and $t = 2s$ a little position error can be observed. This error appears because there is a torque increment at this time, and then the controlled system lost the so called Śsliding modeŠ because the actual sliding gain is too small for

the new uncertainty introduced in the system due to the load torque increment. However, after a short time, the new load torque value is adapted and then the sliding gain value can compensate the system uncertainties, and hence the rotor position error is eliminated. The third graph shows the real and the estimated rotor flux. In this figure it can be observed that the proposed sliding mode observer provides an accurate and fast rotor flux estimation. The fourth graph shows the motor torque, the load torque and the estimated load torque. As it can be seen in this graph, after a transitory time, the load torque observer estimates the load torque value with a small estimation error. This figure also shows that the so-called chattering phenomenon appears in the motor torque. Although this high frequency changes in the torque will be reduced by the mechanical system inertia, they could cause undesirable vibrations in the real rotor, which may be a problem for certain systems. However, for the systems that do not support this chattering, it may be eliminated substituting the sign function by the saturation function in the control signal. The fifth graph shows the stator current i_A. This graph shows that the current signal increases when the load torque increases in order to increment the motor torque. The sixth graph shows the time evolution of the sliding variable. In this figure it can be seen that the system reaches the sliding condition $(S(t) = 0)$ at time $t = 0.25s$, but then the system lost this condition at time $t = 1s$ and $t = 2s$ due to the load torque increment which produces an increment in the system uncertainties.

Figure 5 shows the real test of the variable structure position control using the experimental platform. In this figure, a small noise can be observed in the signals due to the sensors used to make the real measurements in the system. The first graph shows the reference and the real rotor position. Like in the previous case (simulation test), the rotor position tracks the reference position in spite of system uncertainties. The second graph shows the rotor position error. In this experimental validation a small position error is obtained in the presence of a high load torque. It should be noted that this performance is not an easy task to achieve for an induction motor. The third graph shows the estimated rotor flux and the fourth graph shows the motor torque, the load torque and the estimated load torque. It can be noted that the proposed sliding mode observers also perform very well in a practice. The fifth graph shows the stator current i_A, and finally the sixth graph shows the sliding variable S.

6. Conclusion

In this chapter an induction motor position regulation using a sliding mode control for a real-time applications has been presented. In the design a field oriented vector control theory is employed in order to simplify the system dynamic equations.

Additionally, in order to avoid the flux sensors, because the flux sensors increase the cost and reduces the reliability, a rotor flux estimator is proposed. This flux estimator is a sliding mode observer and employs the measured stator voltages and currents in the stationary reference frame. The design incorporates also a load torque observer, based on sliding mode theory, in order to improve the controller performance.

In order to demonstrate the performance of the proposed design over a commercial induction motor of 7.5 kW, a new experimental platform has been designed and constructed in order to text the proposed robust controller in a real time application over a high power commercial induction motor

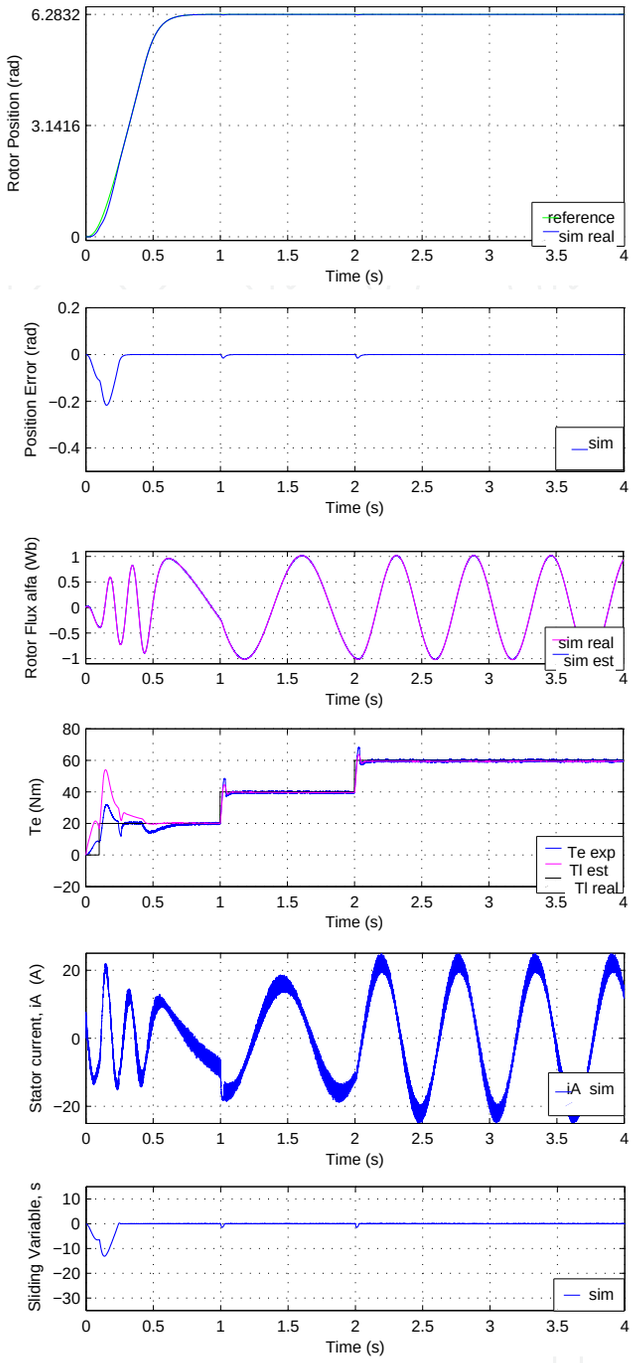

Figure 4. Position tracking simulation results

Due to the nature of the sliding mode control this control scheme is robust under system uncertainties and changes in the load torque applied to the induction motor. The closed loop stability of the presented design has been proved through Lyapunov stability theory.

Finally, by means of simulation and real examples, it has been confirmed that the proposed position control scheme presents a good performance in practice, and that the position tracking objective is achieved under parameter uncertainties and under load torque variations.

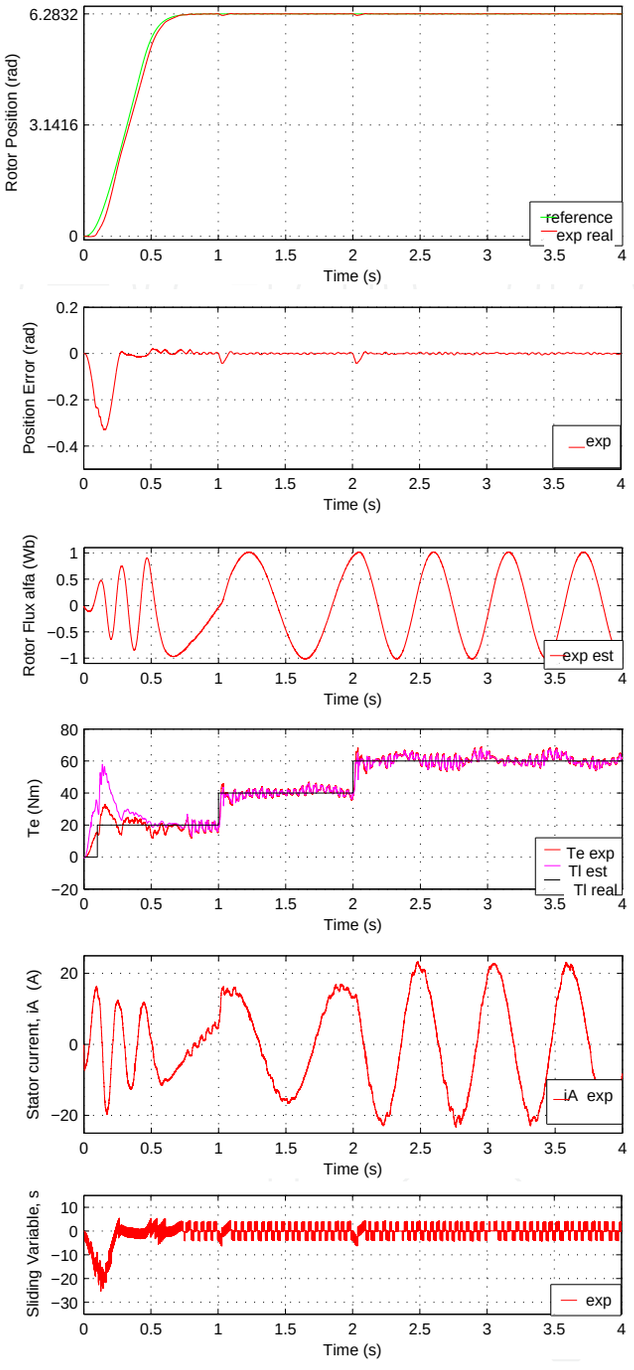

Figure 5. Position tracking experimental results

Acknowledgements

The authors are very grateful to the Basque Government by the support of this work through the project S-PE12UN015 and S-PE13UN039 and to the UPV/EHU by its support through the projects GIU13/41 and UFI11/07.

Author details

Oscar Barambones[1*], Patxi Alkorta[2], Jose M. Gonzalez de Durana[1] and Jose A. Cortajarena[2]

*Address all correspondence to: oscar.barambones@ehu.es

1 Vitoria Engineering School, Vitoria, Spain

2 Eibar Engineering School, Eibar, Spain

References

[1] P. Vas. *Vector Control of AC Machines*. Oxford Science Publications, Oxford. 1994

[2] W. Lehonhard. *Control of Electrical Drives*. Springer, Berlin. 1996

[3] R. Marino, P. Tomei, C.M. Verrelli. (2005) A nonlinear tracking control for sensorless induction motors, *Automatica*, vol. 41, pp. 1071-1077.

[4] R. Yazdanpanah, J. Soltani, G.R. Arab Markadeh. Nonlinear torque and stator flux controller for induction motor drive based on adaptive input-output feedback linearization and sliding mode control *Energy Conversion and Management*, vol. 49, pp. 541-550. 2008

[5] H. Ouadi, F.Giri, A.Elfadili, L.Dugard. (2010) Induction machine speed control with flux optimization, *Control Engineering Practice*, vol. 18, pp. 55-66.

[6] P-H Choua, C-S Chen, F-J Lin. (2012) DSP-based synchronous control of dual linear motors via Sugeno type fuzzy neural network compensator, *Journal of the Franklin Institute*, Vol. 349, pp.792-812.

[7] M.A. Hamidaa, A. Glumineau,n, J. de Leon. (2012) Robust integral backstepping control for sensorless IPM synchronous motor controller, *Journal of the Franklin Institute*, Vol. 349, pp.1734-1757.

[8] V.I. Utkin. Sliding mode control design principles and applications to electric drives, IEEE Trans. Indus. Electro., vol. 40, pp. 26-36. 1993

[9] O. Barambones and P. Alkorta, A robust vector control for induction motor drives with an adaptive sliding-mode control law, Journal of the Franklin Institute, vol. 348, pp. 300-314. 2011

[10] C.-Y Chen, Sliding mode controller design of induction motor based on space-vector pulse width modulation method, Int. J. of Innovative Computing, Information and Control 5, pp. 3603-3614. 2009.

[11] G.R. Lii, C.L. Chiang, C.T. Su and H.R. Hwung. An induction motor position controller optimally designed with fuzzy phase-plane control and genetic algorithms, Electric Power Systems Research, vol. 68, pp. 103-112. 2004.

[12] D. Naso, F. Cupertino and B. Turchiano. Precise position control of tubular linear motors with neural networks and composite learning, Control Engineering Practice, vol. 18, pp. 515-522. 2010.

[13] P. Alkorta, O. Barambones, J.A. Cortajarena, and A. Zubizarrreta, "Efficient Multivariable Generalized Predictive Control for Sensorless Induction Motor Drives", *IEEE Trans. Ind. Electron.*, vol. 61. pp.5126-5134. 2014.

[14] O. Barambones and P. Alkorta,, "Position Control of the Induction Motor using an adaptive sliding mode controller and observers", *IEEE Trans. Ind. Electron.*, vol. 61. pp.6556-6565. 2014.

[15] O. Barambones, P. Alkorta and J.M. Gonzalez de Durana, A real-time estimation and control scheme for induction motors based on sliding mode theory, Journal of the Franklin Institute, vol. 351, pp. 4251-4270. 2014

[16] A. Benchaib and C. Edwards. Nonlinear sliding mode control of an induction motor, *Int. J. of Adaptive Control and Signal Procesing*, vol. 14, pp. 201-221. 2000.

[17] W.J. Wang and J.Y. Chen . Passivity-based sliding mode position control for induction motor drives *IEEE Trans. on Energy conversion*, vol. 20, pp. 316-321. 2005.

[18] B. Veselić, B. Peruničiťć-Draženović, and Č. Milosavljević, High-Performance Position Control of Induction Motor Using Discrete-Time Sliding-Mode Control, *IEEE Trans. Ind. Electron.*, vol. 55, no. 11, pp. 3809-3817, Nov. 2008.

[19] M. Menaa, O. Touhami, R. Ibtiouen and M. Fadel. Sensorless direct vector control of an induction motor, *Control Engineering Practice*, vol. 16, pp. 67-77. 2008

[20] O. Barambones, A.J. Garrido and I. Garrido. (2008) Robust speed estimation and control of an induction motor drive based on artificial neural networks, *Int. J. Adapt. Control Signal Process.*, Vol. 22, pp.440-464.

[21] H. Yang, Y. Xiaa, P. Shi. (2010) Observer-based sliding mode control for a class of discrete systems via delta operator approach, *Journal of the Franklin Institute*, Vol. 347, pp.1199-1213.

[22] A.Y.Alanisa, E.N.Sanchez, A.G.Loukianov, E.A. Hernandez. (2010) Discrete-time recurrent high order neural networks for nonlinear identification, *Journal of the Franklin Institute*, Vol. 347, pp.1253-1265.

[23] B.K. Bose. *Modern Power Electronics and AC Drives.*, Prentice Hall, New Jersey. 2001.

[24] P.V. Kokotovic, H. Khalil, J. OŚReilly. (1996) Singular Perturbation Methods in Control: Analysis and Design *Academic Press*, New York.

[25] O. Barambones, V. Etxebarria, Robust neural control for robotic manipulators, Automatica 38 pp.235-242. 2002